COMPARISON OF IN-PLANE SHEAR BEHAVIORS OF 2-D PLAIN WOVEN C/SiC COMPOSITES

YIQIANG WANG, LITONG ZHANG*, LAIFEI CHENG*

*College of Aeronautical Engineering, Civil Aviation University of China,
Tianjin 300300, People's Republic of China*
**National Key Laboratory of Thermostructure Composite Materials, Northwestern Polytechnical University,
Xi'an Shaanxi, People's Republic of China*

E-mail: wyq80@yahoo.com.cn

The in-plane shear behavior of a plain woven C/SiC composite which exhibits typical ductile tensile behavior (failure strain 0.6-0.8 %) was investigated and compared with that of a brittle plain woven C/SiC composite (tensile failure strain 0.05 %). The shear behavior of ductile composite can be characterized by an initial elastic regime below stress of 40-50 MPa, and a large nonlinear regime followed by a plateau regime up to final failure strain (>2 %), while only the first elastic and last plateau regime can be found for the brittle composite despite that similar shear strain-to-failure and shear knee stresses were found for both ductile and brittle composites. The critical shear stress for matrix cracking was found to be close to the proportional limit stress of ductile composites or strength of brittle ones under uniaxial tensile loading, which could be attributed to the same mechanism of matrix cracks due to the principal tensile stress. Longitudinal intra-yarn cracks and delamination were found for both composites, which could be predominantly responsible for the large shear failure strains observed.

INTRODUCTION

Carbon fiber reinforced silicon carbide matrix composites (C/SiC) have received considerable attention due to their potential commercial applications in jet engine exhaust ducts, leading edges, nose cones and other hot stressed components [1-3]. In most cases these components have to be joined with other metal ones by various joining methods such as riveting, where pin-loaded holes are designed to transfer the mechanical loads and as a consequence, substantial shear stresses are inevitable even when the applied loading is either tensile or compressive [4]. Therefore, an understanding of the shear behavior of this newly-developed material is needed to help make improvements and to design components.

Most previous research has generally focused on the tensile behavior, both monotonic and cyclic, and primary damage mechanisms were summarized including matrix cracking, interface sliding to account for the inelastic strains as well as hysteresis characteristics [5-9]. More recently, efforts has been devoted to the shear behavior, both interlaminar or in-plane [10-12], and these studies indicated that three classes of behavior can be found for the ceramic matrix composites (CMC) based on the

ability to redistribute stress at notches, holes, etc., through inelastic strains that develop upon shear loadings. Up to now the shear behavior of some CMC systems have been investigated, which consist of differing properties of matrix and fibers, such as the low-modulus carbon matrix and high-modulus Al_2O_3, CAS, and SiC matrix composites. However, few attempts dealing with the differences of in-plane shear behavior of 2-D ductile and brittle C/SiC composites have been known to the authors. Thus the current research examines the shear behavior of these two materials and damage mechanisms were addressed to facilitate a constitutive law capable of describing the mechanical behavior of C/SiC components under complex practical loadings.

EXPERIMENTAL

Preparation of C/SiC composites

The reinforcing carbon fiber employed in this study was Torayca T300 (Toray Industries, Inc., Japan), and each yarn contains 1000 fibers. The 2-D fiber preform fabricated by stacking tightly layers of plain woven carbon cloth in an orthogonal way, was supplied by Nanjing Institute of Glass Fiber, People's Republic of China,

and the fiber volume fraction was about 40 % from the vendor. Composite panels were processed by Isothermal chemical vapor infiltration (ICVI) to deposit pyrolytic carbon (PyC) interphase and SiC matrix, which has been described previously [13] and in this study, denoted as CVI PyC+HTT. For the purpose of comparison, a composite without PyC interphase was also fabricated (denoted as Untreated) by directly infiltrating SiC into the fiber preform to cause a strong interface bonding and consequently, a completely brittle tensile behavior is expected for this material. The V-notched Iosipescu shear specimens were cut from the as-infiltrated composite panels and machined to the final shape. Then the SiC coating was deposited on the specimen surfaces with an average thickness of about 100 μm under the same processing conditions to enhance the oxidation resistance. The total shape and dimensions are shown in Figure 1.

Tension tests and microstructural observation

The shear tests were conducted on a conventional Instron 1196 machine under displacement control at a crosshead speed of 0.1 mm/min. Strains were continuously recorded by a two-gauge ±45° rosette which was mounted on the central part between the notches. As shown in Figure 2, an anti-symmetric four point bending fixture was used that a pure shear stress state is induced within the notched section by the application of two counteracting moments produced by two force couples,

$$\tau = \frac{P(a-b)}{wt(a+b)} \qquad (1)$$

where P is the applied maximum load, w is the average specimen width between the notches and t is the thickness, a and b are the distances of the two force couples from the specimen center. More than 5 specimens were tested to check the scatter of the testing results. The shear modulus G was determined from the initial part of shear stress-strain (S-S) curves. The top surface in the gauge section

of the failed specimens was polished and then examined by scanning electron microscopy (SEM, Hitachi S-2700, Japan) to assess the extent of matrix cracking, as well as the fracture surfaces to give information about fiber pullout. For comparison, the corresponding tensile tests were also conducted which have been described previously [13].

RESULTS AND DISCUSSION

The typical monotonic shear stress-strain curves of 2-D woven composites are shown in Figure 3. The curve for the composite with PyC interphase shows an initial elastic behavior below stresses of 40-50 MPa, and then transits to a large nonlinear behavior with continuously decreasing tangent modulus, and finally a softening behavior with an apparent plateau shear stress as the shear strain reaches 2 %. Also shown is the shear curve of composites without PyC interphase for comparison. An initial elastic behavior below stresses of 40-50 MPa was also observed, but almost immediately the curve levels off after this initial elastic behavior, i.e. the large range of nonlinear behavior is absent. The average shear strength of composites with PyC interphase was
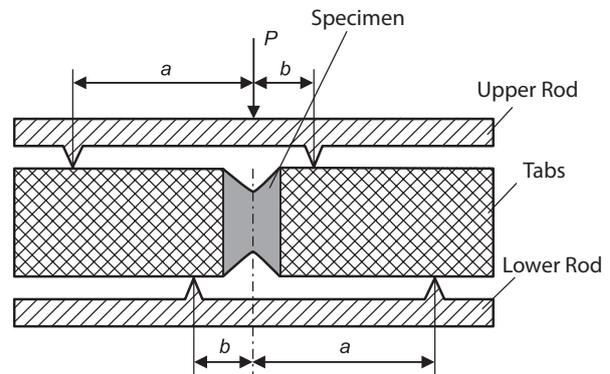

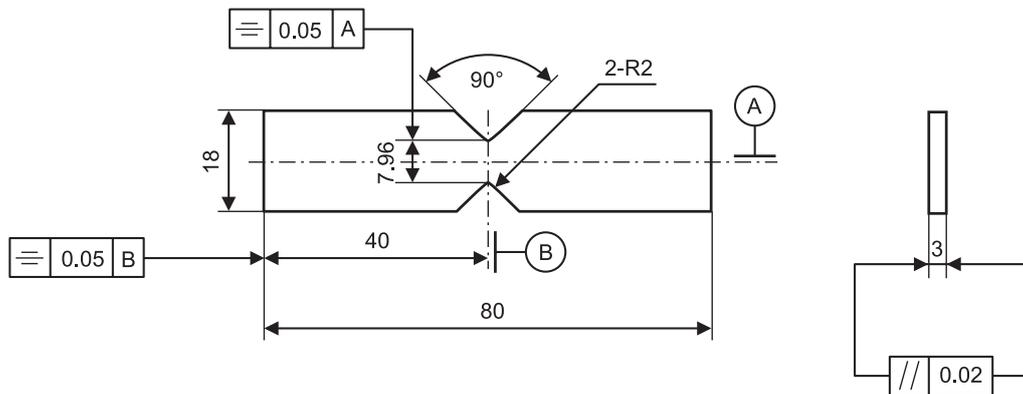Figure 2. Schematic of in-plane shear loading

Figure 1. Configuration of Iosipescu shear specimens.

176 MPa, in contrast to 50 MPa of composites without PyC interphase. However, the shear modulus is not largely influenced and measured as 24-28 GPa for both composites.

Compared to the corresponding tensile behavior (Figure 4), the observed shear strains to failure are significantly larger (2-2.5 %) than the tensile ones (0.6-0.8 % or 0.05 %), no matter whether the material is ductile or brittle. This implies that there exist different damage mechanisms when the composites are subject to shear loadings relative to tensile loadings, such as the well-known multiple matrix cracking normal to the loading direction, interface debonding and sliding, stochastic fiber failure and yarn fracture, since the failure strains of all the constituents (fibers, matrix) are less than 1 %.

Observations on the front face between notches after specimen failure were shown in Figure 5. Matrix cracks were formed both in the outer yarn coating and interior yarns. These cracks, the so-called *en-echelon* microcracks [12], are generally inclined at an average 55° to the loading plane. The crack angle deviation from the theoretical 45° may be related to the mechanical anisotropy of this material, as well as the residual tensile stresses between the warp and weft yarns due to the significant thermal mismatch between carbon fibers and matrix [14]. Nevertheless, the formation and evolution of these cracks signify the onset of the deviation from linearity exhibited in the shear S-S behavior.

The shear knee stresses (40-50 MPa) were found to be similar for both the ductile (CVI PyC+HTT) and brittle (untreated) composites, which are also approximately identical to the proportional limit stress observed for the ductile composites, as well as the tensile strength for the brittle ones, as shown in Figure 4. This phenomenon implies that the mechanism of matrix multiple cracks is the same under shear loadings as under tensile loadings, since the maximum principal tensile stress is equal to the applied shear stress when a unit is subject to pure in-plane shear stress according to the theory of mechanics of materials.

However, only the *en-echelon* matrix crack array cannot account for the fairly large shear strain to failure observed for the present composites. Observations on the fracture surfaces of both composites are shown in Figure 6. It can be seen from the side view that the brittle composites exhibit a planar surface, while the ductile ones show fractured yarns which are apparently inclined due to the shear force and weak yarn/matrix bonding. Longitudinal intra-yarn cracks can be also found for both composites, which were attributed to the reciprocal shear force acting on the yarns along their axes normal to the loading plane, as schematically shown in Figure 7. Thus the composite can be discretized as a series of blocks and it was suggested that the slip between these blocks and rotation between plies lead to the large shear failure strains [15]. Moreover, according to the Halpin-Tsai formula, the shear modulus of a composite can be modeled as

$$G_{12} = \frac{G_f(1+V_f) + G_m(1-V_f)}{G_f(1-V_f) + G_m(1+V_f)} G_m \qquad (2)$$

Since the shear modulus of SiC matrix is greatly larger than that of C fibers (170 vs. 5 GPa) [12, 16], the shear modulus of C/SiC composites is mainly dominated by the matrix. Consequently the severely damaged matrix at high shear stresses would also lead to shear-softening behavior.

CONCLUSIONS

The shear stress-strain behaviors of both ductile and brittle C/SiC composites were compared and various damage modes were identified as responsible for the large inelastic strains. The ductile composites exhibit an
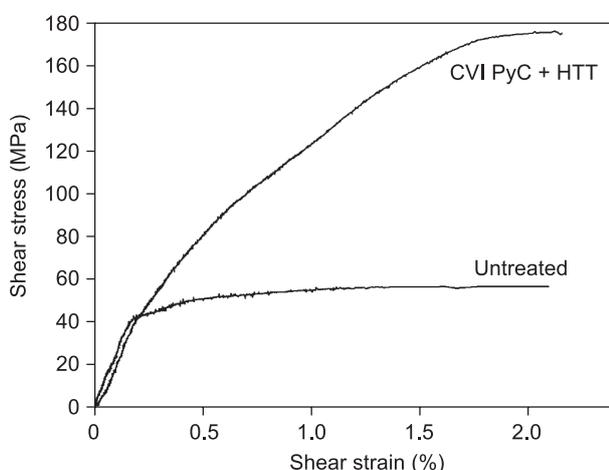

Figure 3. Typical shear stress-strain curves of ductile (denoted CVI PyC+HTT) and brittle (denoted Untreated) plain woven C/SiC composites.
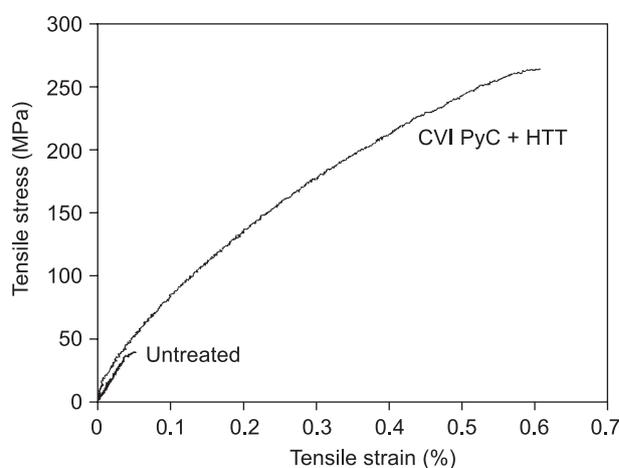

Figure 4. The corresponding tensile stress-strain behaviors of ductile (denoted CVI PyC+HTT) and brittle (denoted Un-treated) plain woven C/SiC composites for comparison.
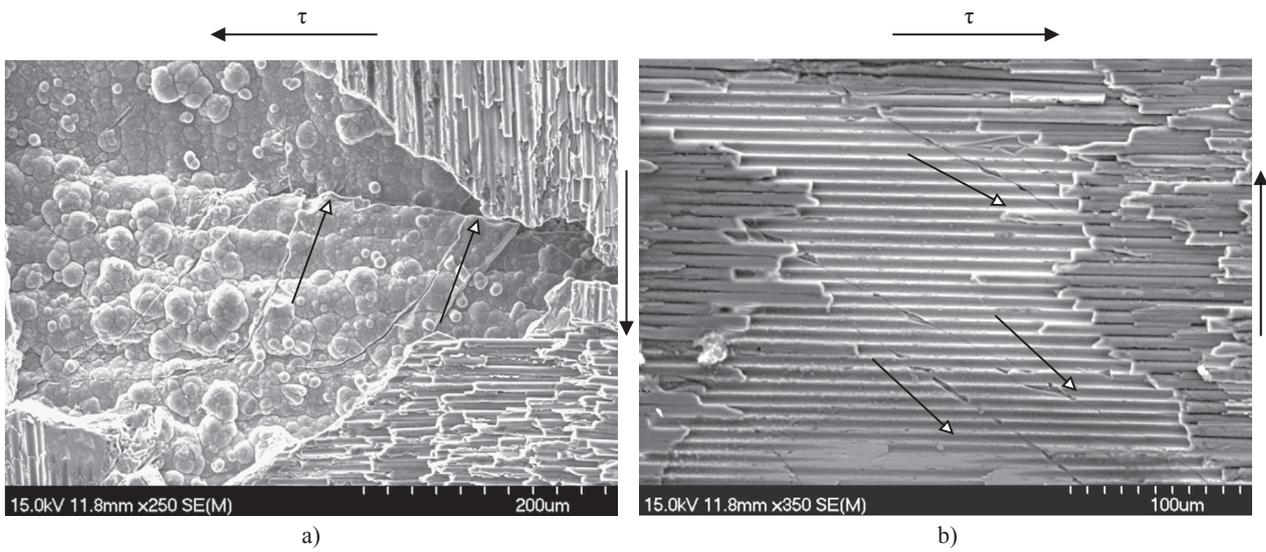
Figure 5. SEM views on the front face between notches after specimen failure showing inclined cracks both in the yarn coating (a) and interior of yarns (b).
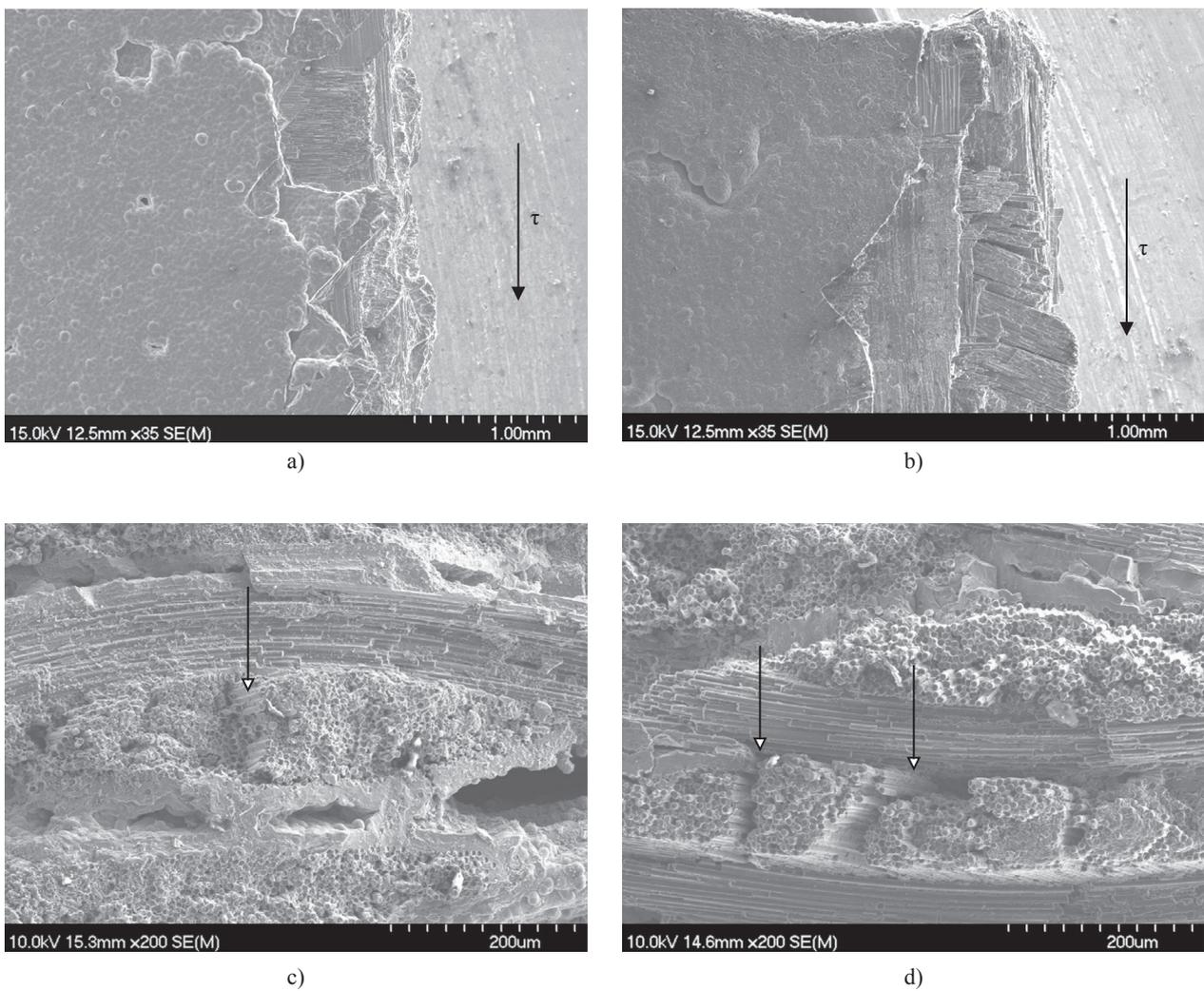

Figure 6. SEM views on the fracture surfaces of brittle composites (a, c) and ductile composites (b, d) showing planar surface for the former, inclined fractured 0° yarns for the latter, and intra-yarn cracks for the both (as arrows indicate).

initial elastic behavior followed by a largely nonlinear behavior, and then a plateau behavior, whereas only the initial elastic behavior and the plateau were exhibited by the brittle composites. However, the shear knee stresses at which the *en-echelon* matrix cracks emerge were found to be the same for both composites. They are also similar to the proportional limit stress for ductile composites or strength for brittle composites under tensile loading, implying the same mechanism of matrix cracks in shear as in tension due to the maximum principal tensile stress. Longitudinal intra-yarn cracks were found for both composites due to the reciprocal shear force, which could be responsible for the large shear failure strains in conjunction with the delamination.
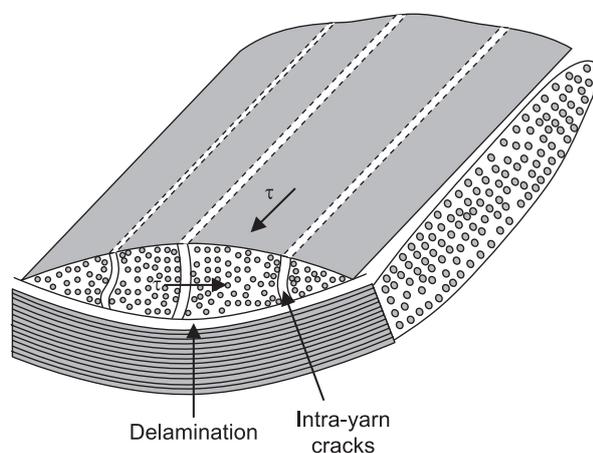

Figure 7. Schematic of damages of plain woven composites under high shear stress showing the longitudinal intra-yarn cracks and delamination.

References

1. Schmidt S, Beyer S, Knabe H, Immich H, Meistring R, Gessler A.: Acta Astronaut. *55*, 409 (2004).
2. Ohnabe H, Masaki S, Onozuka M, Miyahara K, Sasa T.: Composites A *30*, 489 (1999).
3. Naslain R.: Compos. Sci. Technol. *64*, 155 (2004).
4. Brondsted P, Heredia FE, Evans AG.: J. Am. Ceram. Soc. *77*, 2569 (1994).
5. Liu Y, Tanaka Y.: Mater. Lett. *57*, 1571 (2003).
6. Morscher GN.: Compos. Sci. Technol. *64*, 1311 (2004).
7. Lipetzky P, Dvorak GJ, Stoloff NS.: Mater. Sci. Eng. A *216*, 11 (1996).
8. Jacobsen TK, Brondsted P.: J. Am. Ceram. Soc. *84*, 1043 (2001).
9. Koch D, Tushtev K, Grathwohl G.: Compos. Sci. Technol. *68*, 1165 (2008).
10. Fang NJ, Chou T.: J. Am. Ceram. Soc. *76*, 2539 (1993).
11. Cady C, Heredia FE, Evans AG.: J. Am. Ceram. Soc. *78*, 2065 (1995).
12. Turner K. R., Speck J. S., Evans A. G.: J. Am. Ceram. Soc. *78*, 1841 (1995).
13. Wang Y, Zhang L, Cheng L, Mei H, Ma J.: Mater. Sci. Eng. A *497*, 295 (2008).
14. Sbaizero O, Evans AG.: J. Am. Ceram. Soc. *69*, 481(1986).
15. Keith WP, Kedward KT.: J. Am. Ceram. Soc. *80*, 357 (1997).
16. Bertrand S, Forio P, Pailler R.: J. Am. Ceram. Soc. *82*, 2465 (1999).